Simulation of an Induction Motor in the Rotating and Synchronous D/Q Planes

Michael E. Aiello

April 1, 2017

Keywords: Induction Motor, D/Q Plane, Space Harmonic Mutual Inductance Calculations, Coupled-Circuit Model

Abstract

The information provided in this paper is derived entirely from a PhD dissertation written by Paul C. Roberts and submitted to Emmanuel College, University of Cambridge on September 2005 [1]. In his paper Paul C. Roberts provides a detailed theory of operation and practical implementation for a Doubly-Fed Induction (dual stator) machine. This paper is provided only to verify the analysis and findings presented by Paul C. Roberts (hereafter referred to as **Roberts**).

It is highly suggested that the reader review in detail the theory provided by **Roberts** first before referring to the information provided in this paper. This paper for the most part provides only a practical validation to that presented by **Roberts** based on a traditional 3-phase, single stator induction machine.

1 Introduction

Before I attempt to break down the information provided by **Roberts**, it should be mentioned the method used to generate the various simulation provided in this paper. A custom simulation environment was created to provide a means in which to write code (either VHDL implemented in an FPGA or C code implemented in an embedded processor such as DSP) that could run concurrently with the simulation algorithm (sixth order Runge-Kutta). The mechanism for simulation is explained in detail in [4].

2 Representation for a simple 3-Phase, 2-Pole Motor Induction Machine

Roberts presents many different types of dual stator and rotor designs in his paper. Given that this paper does not address dual stator induction motor designs, we can still derive from this pertinent information relative to that of a traditional single stator design.

A somewhat detailed explanation for a 6 bar cage rotor is presented is Section B.7, page 267 of **Roberts**. The details of the stator design are presented in Section B.2.2 page 251. I have provided a verification into the analytical design presentation based on the information provided in Chapter 2 of **Roberts** relative to the 6 bar cage rotor coupled with Stator 1. **Roberts** presents the results of the Stator 1 to Rotor mutual of inductance of this design in Figure B.9-a, page 269 of his paper. My calculations on this same design are shown in Figure 1 below. The results are nearly identical.

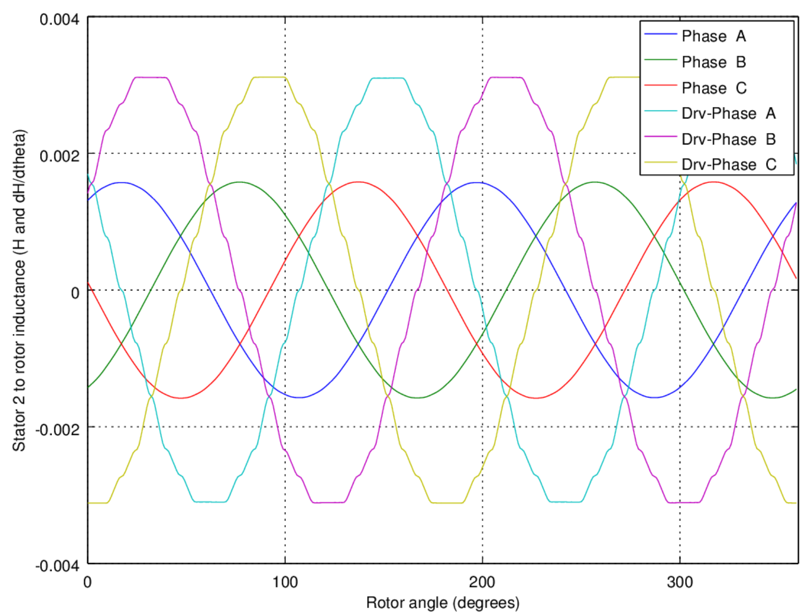

Figure 1: Stator 1 to rotor mutual inductance for BDFM as presented in Figure B.9 (a), page 269 of **Roberts**. Phase A, B, C are the Stator-to-Rotor mutual inductance results for each phase. The derivatives relative to rotor position are also plotted as as Drv-Phase A, Drv-Phase B and Drv-Phase C.

I take these calculations one step further and include the derivative of the three phase coupled mutual inductance relative to rotor position. These calculations were not done in **Roberts**. Note that the design presented by **Roberts** is intended to provide a sinusoidal distribution of the flux within the motor making the assumption that the drive amplifier too be designed to provide sinusoidal output voltage.

For the simulation provided in this paper, I choose to base the stator-rotor design on a somewhat crude winding distribution that would produce CEMF voltages that were essentially *six-step* in appearance. The physical specification for this design and the calculated Stator-Rotor mutual inductance plots are presented in Figures 2, 3 and 4 and Table 1 below.

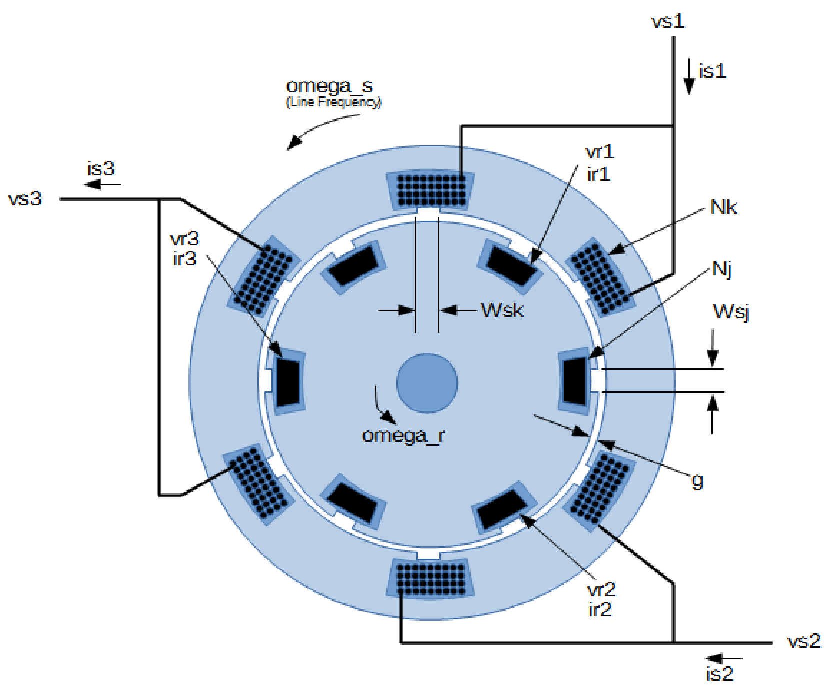

Figure 2: Simplified representation of a 3-phase, 2 pole induction motor used in all simulations provided in this paper.

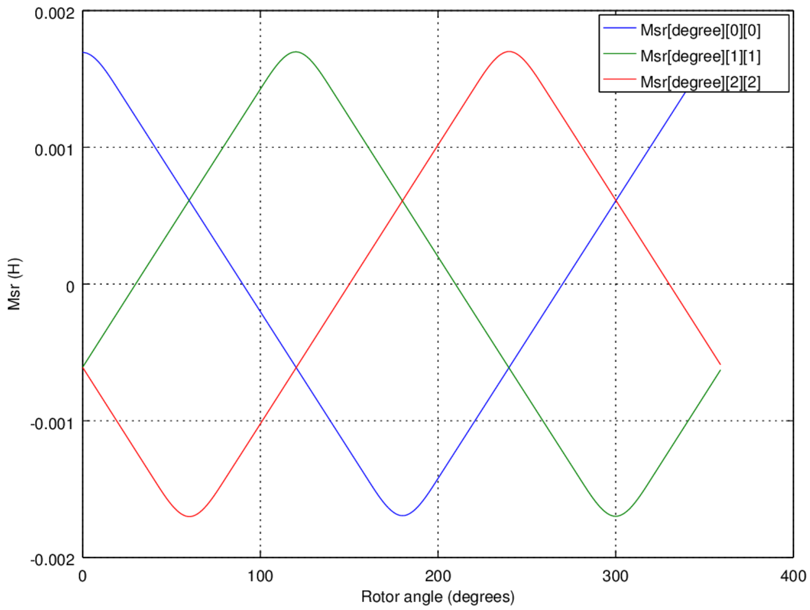

Figure 3: Stator to rotor mutual inductance for the simplified representation of the induction motor described in Figure 2

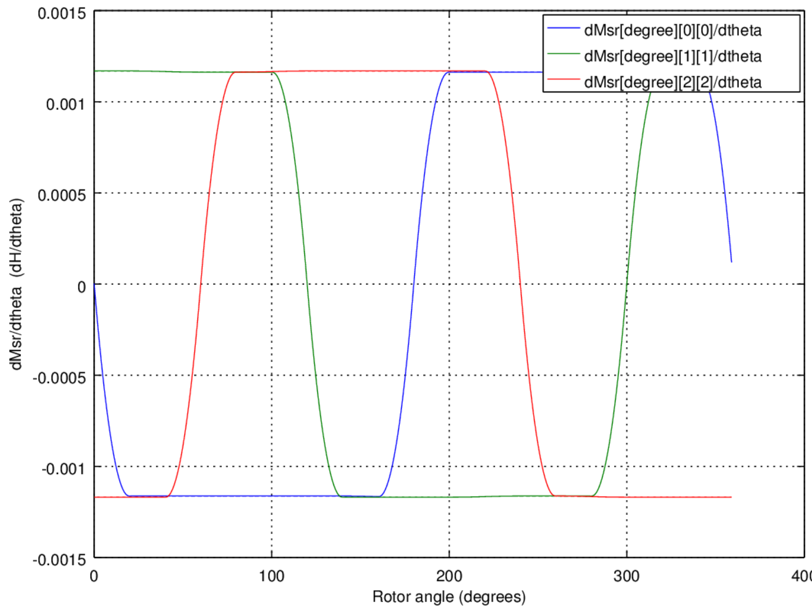

Figure 4: Stator to rotor position derivative mutual inductance for the simplified representation of induction motor described in Figure 2

Parameter	Value
w	.1955 m
d	.1751 m
g	.000555 m
N_k	30.0
N_j	1.0
A_{ck}	PI
W_{sk}	2.0*PI*.03/(2.0*PI*d/2.0)
A_{cj}	PI
W_{sj}	2.0*PI*.03/(2.0*PI*d/2.0)
R_s	2.728 Ω
$R_{r_{loop}}$	.0001 Ω
$R_{r_{bar}}$	-.000025 Ω
J_m	.11 $k_g \cdot m^2$
T_i	.5*ω_r

Table 1: Parameters for the simple induction motor shown in Figure 2 above.

This simplified model of the induction motor serves to illustrate the effect of excessive torque ripple when applying sinusoidal voltages to the terminals. By doing this one can deduce a so called *amount of forgiveness* between a reference model running on the controller and the actual induction motor being controlled.

Before continuing, it should be noted that all simulations presented in this paper are driven by a linear voltage source (linear amplifier) as opposed to a switching PWM source as shown in Figure 5 below.

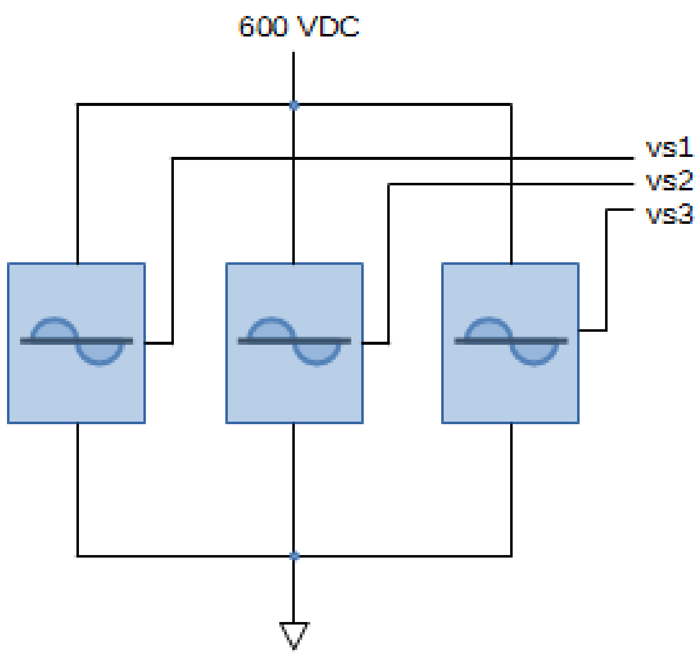

Figure 5: Diagram of voltage source used in this simulation. Only a simple linear amplifier was used to create all simulations presented in this paper. Carrier based PWM and Space-Vector PWM sources could have been used as well (See [4]).

3 Coupled Circuit for the Induction Motor in the physical (Rotating) frame

As per the derivation of the coupled circuit model of the dual stator induction motor given in Equation 2.59 page 66 of **Roberts**, our model for the single stator induction motor is provided by Equations 1 through 3 below.

$$\begin{bmatrix} M_{ss} & M_{sr} \\ M_{sr}^{\intercal} & M_{rr} \end{bmatrix} \begin{bmatrix} \frac{dis}{dt} \\ \frac{dir}{dt} \end{bmatrix} = \left[\begin{bmatrix} vs \\ 0 \end{bmatrix} - \begin{bmatrix} R_s & 0 \\ 0 & R_r \end{bmatrix} - \omega_r \begin{bmatrix} 0 & \frac{dM_{sr}}{dt} \\ \frac{dM_{sr}^{\intercal}}{dt} & 0 \end{bmatrix} \right] \begin{bmatrix} is \\ ir \end{bmatrix} \tag{1}$$

$$\frac{d\theta_r}{dt} = \omega_r \tag{2}$$

$$\frac{d\omega_r}{dt} = \frac{1}{2} \left(\begin{bmatrix} is^{\intercal} & ir^{\intercal} \end{bmatrix} \begin{bmatrix} 0 & \frac{dM_{sr}}{dt} \\ \frac{dM_{sr}^{\intercal}}{dt} & 0 \end{bmatrix} \begin{bmatrix} is \\ ir \end{bmatrix} - T_l \right) / J_m \tag{3}$$

Equations 1 through 3 are expanded in equations 29 through 36 of Appendix A. These equations are presented in a from very close to the code created to run the simulation.

The parameters used in Equations 1 through 3 above are shown in Table 2 as a reference to that derived by **Roberts**.

Of special note are the parameters M_{sr} and $\frac{dM_{sr}}{dt}$. Here, a lookup table with a primary index based on 360 electrical degrees is precomputed for use in the simulator. These lookup tables are shown graphically in Figures 3 and 4 above.

Parameter	Deriving reference	Page Number	Notes
M_{ss}	Eq. 2.27 and 2.44	46 and 56	
M_{sr}	Eq. 2.27 and 2.53	46 and 63	Matrix array created by 360 iterations.
M_{rr}	Eq. 2.27 and 2.51	46 and 62	
R_s			A simple diagonal of phase resistance.
R_r	Section B.8	267	Connections between bars are included.
$\frac{dM_{sr}}{dt}$	Eq. 2.27 and 2.53	46 and 63	360 iterations of the derivative of Eq. 2.27

Table 2: Reference to the parameters in the rotating frame as defined by **Roberts**.

4 Coupled Circuit for the Induction Motor in the D/Q (slip) frame

Unlike the synchronous motor, a simple translation from the rotating (or terminal) plane to the D/Q plane for an induction motor places the point of reference relative to the *slip* frequency of the motor. The D/Q transformation is described beginning in Chapter 3 page 69 of **Roberts**.

For our simplified single stator motor, the D/Q transformation of Equations 1 through 3 are described by Equations 4 through 6 below.

$$\begin{bmatrix} M_{dq0s} & M_{dqsr} \\ M_{dqsr}^{\intercal} & M_{dqr} \end{bmatrix} \begin{bmatrix} \frac{dis_{dq}}{dt} \\ \frac{dir_{dq}}{dt} \end{bmatrix} = \begin{bmatrix} vs_{dq} \\ 0 \end{bmatrix} - \left[\begin{bmatrix} R_{dq0s} & 0 \\ 0 & R_{dqr} \end{bmatrix} - \omega_r \begin{bmatrix} Q_{dq0s} & Q_{dqsr} \\ 0 & 0 \end{bmatrix} \right] \begin{bmatrix} is_{dq} \\ ir_{dq} \end{bmatrix} \tag{4}$$

$$\frac{d\theta_r}{dt} = \omega_r \tag{5}$$

$$\frac{d\omega_r}{dt} = \frac{1}{2} \left(\begin{bmatrix} is_{dq}^{\intercal} & ir_{dq}^{\intercal} \end{bmatrix} \begin{bmatrix} 0 & Q_{dqsr} \\ Q_{dqsr}^{\intercal} & 0 \end{bmatrix} \begin{bmatrix} is_{dq} \\ ir_{dq} \end{bmatrix} - T_l \right) / J_m \tag{6}$$

Similar to that done for the rotating plane, Equations 4 through 6 are expanded in equations 37 through 44 of Appendix A. However because we are not yet in the proper reference plane suitable as a bases for controlling the motor, simulation in this reference plane is not presented in this paper.

In any event, the parameters used in Equations 4 through 6 are shown in Table 3 below as a reference to that derived by **Roberts**.

Parameter	Deriving reference	Page Number
M_{dq0s}	Eq. 3.19	76
M_{dqsr}	Eq. 3.26	79
M_{dqr}	Eq. 3.24	77
R_{dq0s}	Unchanged from R_s by D/Q transformation.	
R_{dqr}	Diagonalized by D/Q transformation applied to R_r.	
Q_{dq0s}	Eq. 3.17	76
Q_{dqsr}	Eq. 3.28	79

Table 3: Reference to the parameters in the D/Q frame as defined by Roberts.

5 Coupled Circuit for the Induction Motor in the Synchronous D/Q frame

As pointed out in **Roberts** Section 7.2 page 176, one additional transformation needs to be preformed on the equations establishing the *slip* frame to make the model usable for control. By doing this, we now are similar to the D/Q reference frame that would be established when evaluating the coupled equations for permanent magnet synchronous machine (see [2] and [4]).

For our simplified single stator motor, the Synchronous D/Q transformation of Equations 4 through 6 are described by Equations 7 through 9 below.

$$\begin{aligned}\begin{bmatrix} M_{sync0s} & M_{syncsr} \\ M_{syncsr}^{\intercal} & M_{syncr} \end{bmatrix} \begin{bmatrix} \frac{dis_{sdq}}{dt} \\ \frac{dir_{sdq}}{dt} \end{bmatrix} = \\ \begin{bmatrix} vs_{sdq} \\ 0 \end{bmatrix} - \begin{bmatrix} \begin{bmatrix} R_{sync0s} & 0 \\ 0 & R_{syncr} \end{bmatrix} - \omega_r \begin{bmatrix} Q_{sync0s} & Q_{syncsr} \\ 0 & 0 \end{bmatrix} \\ -(\omega_r - \omega_s) \begin{bmatrix} Q_{syncd0s} & Q_{syncdsr} \\ Q_{syncdsr}^{\intercal} & Q_{syncdr} \end{bmatrix} \end{bmatrix} \begin{bmatrix} is_{sdq} \\ ir_{sdq} \end{bmatrix}\end{aligned} \tag{7}$$

$$\frac{d\theta_r}{dt} = \omega_r \tag{8}$$

$$\frac{d\omega_r}{dt} = \frac{1}{2} \left(\begin{bmatrix} is_{sdq}^{\intercal} & ir_{sdq}^{\intercal} \end{bmatrix} \begin{bmatrix} 0 & S_{syncsr} \\ S_{syncsr}^{\intercal} & 0 \end{bmatrix} \begin{bmatrix} is_{sdq} \\ ir_{sdq} \end{bmatrix} - T_l \right) / J_m \tag{9}$$

Similar to that done for the rotating plane and D/Q (*slip*) frames above, Equations 7 through 9 are expanded in equations 45 through 52 of Appendix A.

The parameters used in Equations 7 through 9 are shown in Table 4 below as a reference to that derived by **Roberts**.

Parameter	Deriving reference	Page Number
M_{sync0s}	Top left element of M_{sync}, Eq. 7.9	179
M_{syncsr}	Top right element of M_{sync}, Eq. 7.9	179
$M^{\intercal}_{syncsr}$	Bottom left element of M_{sync}, Eq. 7.9	179
M_{syncr}	Bottom right element of M_{sync}, Eq. 7.9	179
R_{sync0s}	Top left element of R_{sync}, Eq. 7.7	179
R_{syncr}	Bottom right element of R_{sync}, Eq. 7.7	179
Q_{sync0s}	Top left element, first term of Q_{sync}, Eq. 7.8	179
Q_{syncsr}	Top right element, first term of Q_{sync}, Eq. 7.8	179
$Q_{syncd0s}$	Top left element, second term of Q_{sync}, Eq. 7.8	179
$Q_{syncdsr}$	Top right element, second term of Q_{sync}, Eq. 7.8	179
$Q^{\intercal}_{syncdsr}$	Bottom left element, second term of Q_{sync}, Eq. 7.8	179
Q_{syncdr}	Bottom right element, second term of Q_{sync}, Eq. 7.8	179
S_{syncsr}	Top right element of S_{sync}, Eq. 7.10	179
$S^{\intercal}_{syncsr}$	Bottom left element of S_{sync}, Eq. 7.10	179

Table 4: Reference to the parameters in the synchronous D/Q frame as defined by **Roberts**

6 Feedback Linearization

Some control strategies for the dual stator induction motor are suggested by **Roberts** (review Chapter 7 and 8). Obviously the approaches he derives for the BDFM can be applied to the a standard single stator induction motor using very simple modifications. Before continuing, it should be noted that **Roberts** simplifies the derivation for the motor equations in the D/Q *slip* plane so as to remove some of the zero sequence terms (see Equation 3.30, page 80 of his paper).

I go one step further and set the condition that the motor windings are balanced allowing all zero sequence terms to be removed from the equations derived so far. This is denoted by the *bar* placed above all parameters (for example $\overline{M}_{syncsr}$).

Using the references defined in Table 4 above, define the modified matrix definitions created by multiplying through by the inverse of the matrix $\overline{M}_{sync}$. The results are shown in equations 10 through 12.

$$\overline{R}_{sync\_m} = \begin{bmatrix} \overline{M}_{sync0s} & \overline{M}_{syncsr} \\ \overline{M^{\intercal}}_{syncsr} & \overline{M}_{syncr} \end{bmatrix}^{-1} \begin{bmatrix} \overline{R}_{sync0s} & 0 \\ 0 & \overline{R}_{syncr} \end{bmatrix} \tag{10}$$

$$\overline{Q}_{sync\_m} = \begin{bmatrix} \overline{M}_{sync0s} & \overline{M}_{syncsr} \\ \overline{M^{\intercal}}_{syncsr} & \overline{M}_{syncr} \end{bmatrix}^{-1} \begin{bmatrix} \overline{Q}_{sync0s} & \overline{Q}_{syncsr} \\ 0 & 0 \end{bmatrix} \tag{11}$$

$$\overline{Q}_{syncd\_m} = \begin{bmatrix} \overline{M}_{sync0s} & \overline{M}_{syncsr} \\ \overline{M^{\intercal}}_{syncsr} & \overline{M}_{syncr} \end{bmatrix}^{-1} \begin{bmatrix} \overline{Q}_{syncd0s} & \overline{Q}_{syncdsr} \\ \overline{Q^{\intercal}}_{syncdsr} & \overline{Q}_{syncdr} \end{bmatrix} \tag{12}$$

The inverse of the matrix $\overline{M}_{sync}$ is defined by equation 13.

$$\overline{M}_{sync\_inv} = \begin{bmatrix} \overline{M}_{sync0s} & \overline{M}_{syncsr} \\ \overline{M^{\intercal}}_{syncsr} & \overline{M}_{syncr} \end{bmatrix}^{-1} \tag{13}$$

Using equations 10 through 13, Equation 7 is transformed to Equation 14 below.

$$\begin{bmatrix} \frac{dis_{sdqd}}{dt} \\ \frac{dis_{sdqq}}{dt} \\ \frac{dir_{sdqd}}{dt} \\ \frac{dir_{sdqq}}{dt} \end{bmatrix} = \begin{bmatrix} vs_{sdqd}\overline{M}_{sync\_inv[0][0]} \\ vs_{sdqq}\overline{M}_{sync\_inv[1][1]} \\ vs_{sdqd}\overline{M}_{sync\_inv[2][0]} \\ vs_{sdqq}\overline{M}_{sync\_inv[3][1]} \end{bmatrix} - \begin{bmatrix} \overline{R}_{sync\_m} - \omega_r \overline{Q}_{sync\_m} \\ -(\omega_r - \omega_s)\overline{Q}_{syncd\_m} \end{bmatrix} \begin{bmatrix} is_{sdqd} \\ is_{sdqq} \\ ir_{sdqd} \\ ir_{sdqq} \end{bmatrix} \tag{14}$$

Next, define a new matrix $\overline{T}_{sync}$ as described by equation 15 below.

$$\overline{T}_{sync} = \begin{bmatrix} 0 & \overline{S}_{syncsr} \\ \overline{S^{\intercal}}_{syncsr} & 0 \end{bmatrix}^{-1} \begin{bmatrix} \overline{M}_{sync0s} & \overline{M}_{syncsr} \\ \overline{M^{\intercal}}_{syncsr} & \overline{M}_{syncr} \end{bmatrix} \tag{15}$$

Again, using the definitions provided by Table 4 above, define a new set of transformation matrices as described by equations 16 through 18 below.

$$\overline{R}_{sync\_c} = \overline{T}_{sync} \begin{bmatrix} \overline{R}_{sync0s} & 0 \\ 0 & \overline{R}_{syncr} \end{bmatrix} \tag{16}$$

$$\overline{Q}_{sync\_c} = \overline{T}_{sync} \begin{bmatrix} \overline{Q}_{sync0s} & \overline{Q}_{syncsr} \\ 0 & 0 \end{bmatrix} \tag{17}$$

$$\overline{Q}_{syncd\_c} = \overline{T}_{sync} \begin{bmatrix} \overline{Q}_{syncd0s} & \overline{Q}_{syncdsr} \\ \overline{Q^{\intercal}}_{syncdsr} & \overline{Q}_{syncdr} \end{bmatrix} \tag{18}$$

Stator voltages to be applied to the motor can now be determined. Based on the motor model for single stator winding, equation (8.14) on page 213 of **Roberts** can be expanded as shown in equation 19 below.

$$\begin{aligned}
is_{sdqd}vs_{sdqq}\overline{T}_{sync[0][1]} + is_{sdqq}vs_{sdqd}\overline{T}_{sync[1][0]} + \\
ir_{sdqd}vs_{sdqq}\overline{T}_{sync[2][1]} + ir_{sdqq}vs_{sdqd}\overline{T}_{sync[3][0]} - \\
is_{sdqd}(is_{sdqq}\overline{R}_{sync_c[0][1]} + ir_{sdqq}\overline{R}_{sync_c[0][3]}) - \\
is_{sdqq}(is_{sdqd}\overline{R}_{sync_c[1][0]} + ir_{sdqd}\overline{R}_{sync_c[1][2]}) - \\
ir_{sdqd}(is_{sdqq}\overline{R}_{sync_c[2][1]} + ir_{sdqq}\overline{R}_{sync_c[2][3]}) - \\
ir_{sdqq}(is_{sdqd}\overline{R}_{sync_c[3][0]} + ir_{sdqd}\overline{R}_{sync_c[3][2]}) - \\
(is_{sdqd}^2\overline{Q}_{sync_c[0][0]} + is_{sdqd}ir_{sdqd}\overline{Q}_{sync_c[0][2]} + \\
is_{sdqq}^2\overline{Q}_{sync_c[1][1]} + is_{sdqq}ir_{sdqq}\overline{Q}_{sync_c[1][3]} + \\
ir_{sdqd}is_{sdqd}\overline{Q}_{sync_c[2][0]} + ir_{sdqd}^2\overline{Q}_{sync_c[2][2]} + \\
ir_{sdqq}is_{sdqq}\overline{Q}_{sync_c[3][1]} + ir_{sdqq}^2\overline{Q}_{sync_c[3][3]})\omega_r - \\
(is_{sdqd}^2\overline{Q}_{syncd_c[0][0]} + is_{sdqd}ir_{sdqd}\overline{Q}_{syncd_c[0][2]} + \\
is_{sdqq}^2\overline{Q}_{syncd_c[1][1]} + is_{sdqq}ir_{sdqq}\overline{Q}_{syncd_c[1][3]} + \\
ir_{sdqd}is_{sdqd}\overline{Q}_{syncd_c[2][0]} + ir_{sdqd}^2\overline{Q}_{syncd_c[2][2]} + \\
ir_{sdqq}is_{sdqq}\overline{Q}_{syncd_c[3][1]} + ir_{sdqq}^2\overline{Q}_{syncd_c[3][3]})(\omega_r - \omega_s) - \\
Jm\frac{d^2\omega_r}{dt^2} - Bm\frac{d\omega_r}{dt} = 0
\end{aligned} \tag{19}$$

Roberts does not elaborate on what type of minimization should be done to vs_{sdqd} and vs_{sdqq} to obtain a solution for equation 19. I believe he is referring to the use of Lagrange Multipliers for which the method to determine a minimum for the vector vs_{sdq} is described in [2] using the constraint that the quantity $vs_{sdqd}^2 + s_{sdqq}^2$ be held to a minimum around a unit circle. Information for this method can also be found by referring to [3], Chapter 4.

This in my opinion is too general of a constraint in that this approach ignores the unit current stress on the amplifier element (the servo drive power stage) for the sake of keeping the magnitude of the voltage to a minimum (see [4] Section B.1.3).

Instead, vs_{sdqd} and vs_{sdqq} should be considered independent of each other where in a closed loop control environment, vs_{sdqq} is responsible for torque control with vs_{sdqd} uses to control motor flux.

7 The Lagrange method applied to the Induction Motor electrical model.

Equation 19 contains three unknown control variables, the applied stator voltages vs_{sdqd}, vs_{sdqq}, and ω_s the driving frequency for these stator voltages.

The Lagrange method mentioned in the previous section can be used to determine the value vs_{sdqq} and ω_s while leaving vs_{sdqd} as the independent variable for controlling motor flux. Normally, we would set vs_{sdqd} to zero while determining vs_{sdqq} and ω_s. But as will be mentioned in Section B.1 below, the open loop voltage generating equations used in this simulation produced the driving voltage on vs_{sdqd} with vs_{sdqq} set to zero.

So in order to adjust for this we will set vs_{sdqq} to zero and derive vs_{sdqd} and ω_s instead. Applying the Lagrange we obtain the following results [1].

Define row number one of equation 14 with $\frac{dis_{sdqd}}{dt}$ set to zero as.
$f_1(vs_{sdqd}, vs_{sdqq}, is_{sdqd}, is_{sdqq}, ir_{sdqd}, ir_{sdqq}, \omega_r, \omega_s) = 0$

Define row number two of equation 14 with $\frac{dis_{sdqq}}{dt}$ set to zero as.
$f_2(vs_{sdqd}, vs_{sdqq}, is_{sdqd}, is_{sdqq}, ir_{sdqd}, ir_{sdqq}, \omega_r, \omega_s) = 0$

Define row number three of equation 14 with $\frac{dir_{sdqd}}{dt}$ set to zero as.
$f_3(vs_{sdqd}, vs_{sdqq}, is_{sdqd}, is_{sdqq}, ir_{sdqd}, ir_{sdqq}, \omega_r, \omega_s) = 0$

Define row number four of equation 14 with $\frac{dir_{sdqq}}{dt}$ set to zero as.
$f_4(vs_{sdqd}, vs_{sdqq}, is_{sdqd}, is_{sdqq}, ir_{sdqd}, ir_{sdqq}, \omega_r, \omega_s) = 0$

Define the constraint equation as:

$$\begin{aligned} g(vs_{sdqd}, vs_{sdqq}, is_{sdqd}, is_{sdqq}, ir_{sdqd}, ir_{sdqq}, \omega_r, \omega_s) = \\ vs_{sdqd}^2 + vs_{sdqq}^2 + C \end{aligned} \tag{20}$$

Construct the set of Lagrange multipliers as described in equations 21 through 28 below.

$$\begin{aligned} k_1\frac{\partial f_1}{\partial vs_{sdqd}} + k2\frac{\partial f_2}{\partial vs_{sdqd}} + k_3\frac{\partial f_3}{\partial vs_{sdqd}} + k4\frac{\partial f_4}{\partial vs_{sdqd}} = \frac{\partial g}{\partial vs_{sdqd}} \\ k_1\overline{M}_{sync\_inv[0][0]} + k_3\overline{M}_{sync\_inv[2][0]} = 2vs_{sdqd} \end{aligned} \tag{21}$$

[1] In open loop, vs_{sdqq} and vs_{sdqd} do not have any direct representation as to the component that produces torque or control flux

$$k_1\frac{\partial f_1}{\partial vs_{sdqq}} + k2\frac{\partial f_2}{\partial vs_{sdqq}} + k_3\frac{\partial f_3}{\partial vs_{sdqq}} + k4\frac{\partial f_4}{\partial vs_{sdqq}} = \frac{\partial g}{\partial vs_{sdqq}} \\ k_2\overline{M}_{sync\_inv[1][1]} + k_3\overline{M}_{sync\_inv[3][1]} = 2vs_{sdqq} \tag{22}$$

$$k_1\frac{\partial f_1}{\partial is_{sdqd}} + k2\frac{\partial f_2}{\partial is_{sdqd}} + k_3\frac{\partial f_3}{\partial is_{sdqd}} + k4\frac{\partial f_4}{\partial is_{sdqd}} = \frac{\partial g}{\partial is_{sdqd}} \\ -k_1\overline{R}_{sync\_m[0][0]} - \\ k_2\omega_r(\overline{Q}_{sync\_m[1][0]} + \overline{Q}_{syncd\_m[1][0]}) + \\ k_2\omega_s\overline{Q}_{syncd\_m[1][0]} - \\ k_3\overline{R}_{sync\_m[2][0]} - \\ k_4\omega_r(\overline{Q}_{sync\_m[3][0]} + \overline{Q}_{syncd\_m[3][0]}) + \\ k_4\omega_s\overline{Q}_{syncd\_m[3][0]} = \\ 0 \tag{23}$$

$$k_1\frac{\partial f_1}{\partial is_{sdqq}} + k2\frac{\partial f_2}{\partial is_{sdqq}} + k_3\frac{\partial f_3}{\partial is_{sdqq}} + k4\frac{\partial f_4}{\partial is_{sdqq}} = \frac{\partial g}{\partial is_{sdqq}} \\ -k_1\omega_r(\overline{Q}_{sync\_m[0][1]} + \overline{Q}_{syncd\_m[0][1]}) + \\ k_1\omega_s\overline{Q}_{syncd\_m[0][1]} - \\ k_2\overline{R}_{sync\_m[1][1]} - \\ k_3\omega_r(\overline{Q}_{sync\_m[2][1]} + \overline{Q}_{syncd\_m[2][1]}) + \\ k_3\omega_s\overline{Q}_{syncd\_m[2][1]} - \\ k_4\overline{R}_{sync\_m[3][1]} = \\ 0 \tag{24}$$

$$k_1\frac{\partial f_1}{\partial ir_{sdqd}} + k2\frac{\partial f_2}{\partial ir_{sdqd}} + k_3\frac{\partial f_3}{\partial ir_{sdqd}} + k4\frac{\partial f_4}{\partial ir_{sdqd}} = \frac{\partial g}{\partial ir_{sdqd}} \\ -k_1\overline{R}_{sync\_m[0][2]} - \\ k_2\omega_r(\overline{Q}_{sync\_m[1][2]} + \overline{Q}_{syncd\_m[1][2]}) + \\ k_2\omega_s\overline{Q}_{syncd\_m[1][2]} - \\ k_3\overline{R}_{sync\_m[2][2]} - \\ k_4\omega_r(\overline{Q}_{sync\_m[3][2]} + \overline{Q}_{syncd\_m[3][2]}) + \\ k_4\omega_s\overline{Q}_{syncd\_m[3][2]} = \\ 0 \tag{25}$$

$$k_1\frac{\partial f_1}{\partial ir_{sdqq}} + k2\frac{\partial f_2}{\partial ir_{sdqq}} + k_3\frac{\partial f_3}{\partial ir_{sdqq}} + k4\frac{\partial f_4}{\partial ir_{sdqq}} = \frac{\partial g}{\partial ir_{sdqq}} \\ -k_1\omega_r(\overline{Q}_{sync\_m[0][3]} + \overline{Q}_{syncd\_m[0][3]})+ \\ k_1\omega_s\overline{Q}_{syncd\_m[0][3]}- \\ k_2\overline{R}_{sync\_m[1][3]}- \\ k_3\omega_r(\overline{Q}_{sync\_m[2][3]} + \overline{Q}_{syncd\_m[2][3]})+ \\ k_3\omega_s\overline{Q}_{syncd\_m[2][3]}- \\ k_4\overline{R}_{sync\_m[3][3]} = \\ 0 \tag{26}$$

$$k_1\frac{\partial f_1}{\partial \omega_r} + k2\frac{\partial f_2}{\partial \omega_r} + k_3\frac{\partial f_3}{\partial \omega_r} + k4\frac{\partial f_4}{\partial \omega_r} = \frac{\partial g}{\partial \omega_r} \\ -k_1(is_{sdqq}(\overline{Q}_{sync\_m[0][1]} + \overline{Q}_{syncd\_m[0][1]})+ \\ ir_{sdqq}(\overline{Q}_{sync\_m[0][3]} + \overline{Q}_{syncd\_m[0][3]})- \\ k_2(is_{sdqd}(\overline{Q}_{sync\_m[1][0]} + \overline{Q}_{syncd\_m[1][0]})+ \\ ir_{sdqd}(\overline{Q}_{sync\_m[1][2]} + \overline{Q}_{syncd\_m[1][2]})- \\ k_3(is_{sdqq}(\overline{Q}_{sync\_m[2][1]} + \overline{Q}_{syncd\_m[2][1]})+ \\ ir_{sdqq}(\overline{Q}_{sync\_m[2][3]} + \overline{Q}_{syncd\_m[2][3]})- \\ k_4(is_{sdqd}(\overline{Q}_{sync\_m[3][0]} + \overline{Q}_{syncd\_m[3][0]})+ \\ ir_{sdqd}(\overline{Q}_{sync\_m[3][2]} + \overline{Q}_{syncd\_m[3][2]}) = \\ 0 \tag{27}$$

$$k_1\frac{\partial f_1}{\partial \omega_s} + k2\frac{\partial f_2}{\partial \omega_s} + k_3\frac{\partial f_3}{\partial \omega_s} + k4\frac{\partial f_4}{\partial \omega_s} = \frac{\partial g}{\partial \omega_s} \\ k_1(is_{sdqq}\overline{Q}_{syncd\_m[0][1]} + ir_{sdqq}\overline{Q}_{syncd\_m[0][3]})+ \\ k_2(is_{sdqd}\overline{Q}_{syncd\_m[1][0]} + ir_{sdqd}\overline{Q}_{syncd\_m[1][2]})+ \\ k_3(is_{sdqq}\overline{Q}_{syncd\_m[2][1]} + ir_{sdqq}\overline{Q}_{syncd\_m[2][3]})+ \\ k_4(is_{sdqd}\overline{Q}_{syncd\_m[3][0]} + ir_{sdqd}\overline{Q}_{syncd\_m[3][2]}) = \\ 0 \tag{28}$$

Using Equations 14, 21, 22, 27 and 28 solve for vs_{sdqd} and ω_s. The results of this verification are shown in Figure 21 of Section B.4.

A The Expanded Coupled Circuit Model for the Induction Motor

The circuit models for the induction motor described by Equations 1 through 3, 4 through 6 and 7 through 9 must be flattened before being processes by the simulator. This expansion is shown in the following subsections A.1, A.3 and A.3 for rotating model, the D/Q (slip) model and the Synchronous D/Q model respectively. As mentioned previously only the simulations for the rotating frame and the Synchronous D/Q frame are presented in this paper.

A.1 Expansion in the rotating frame

The expansion of equations 1) through 3 is provided in equations 29 through 36 below.

$$\begin{aligned}
M_{ss[0][0]}\frac{dis_1}{dt} + M_{ss[0][1]}\frac{dis_2}{dt} + M_{ss[0][2]}\frac{dis_3}{dt} \\
+M_{sr[\theta_r][0][0]}\frac{dir_1}{dt} + M_{sr[\theta_r][0][1]}\frac{dir_2}{dt} + M_{sr[\theta_r][0][2]}\frac{dir_3}{dt} &= \\
vs_1 - R_{s[0][0]}is_1 \\
-\omega_r(\frac{dM_{sr[\theta_r][0][0]}}{d\theta_r}ir_1 + \frac{dM_{sr[\theta_r][0][1]}}{d\theta_r}ir_2 + \frac{dM_{sr[\theta_r][0][2]}}{d\theta_r}ir_3)
\end{aligned} \tag{29}$$

$$\begin{aligned}
M_{ss[1][0]}\frac{dis_1}{dt} + M_{ss[1][1]}\frac{dis_2}{dt} + M_{ss[1][2]}\frac{dis_3}{dt} \\
+M_{sr[\theta_r][1][0]}\frac{dir_1}{dt} + M_{sr[\theta_r][1][1]}\frac{dir_2}{dt} + M_{sr[\theta_r][1][2]}\frac{dir_3}{dt} &= \\
vs_2 - R_{s[1][1]}is_2 \\
-\omega_r(\frac{dM_{sr[\theta_r][1][0]}}{d\theta_r}ir_1 + \frac{dM_{sr[\theta_r][1][1]}}{d\theta_r}ir_2 + \frac{dM_{sr[\theta_r][1][2]}}{d\theta_r}ir_3)
\end{aligned} \tag{30}$$

$$\begin{aligned}
M_{ss[2][0]}\frac{dis_1}{dt} + M_{ss[2][1]}\frac{dis_2}{dt} + M_{ss[2][2]}\frac{dis_3}{dt} \\
+M_{sr[\theta_r][2][0]}\frac{dir_1}{dt} + M_{sr[\theta_r][2][1]}\frac{dir_2}{dt} + M_{sr[\theta_r][2][2]}\frac{dir_3}{dt} &= \\
vs_3 - R_{s[2][2]}is_{_3} \\
-\omega_r(\frac{dM_{sr[\theta_r][2][0]}}{d\theta_r}ir_1 + \frac{dM_{sr[\theta_r][2][1]}}{d\theta_r}ir_2 + \frac{dM_{sr[\theta_r][2][2]}}{d\theta_r}ir_3)
\end{aligned} \tag{31}$$

$$
\begin{aligned}
M_{sr[\theta_r][0][0]}\frac{dis_1}{dt} + M_{sr[\theta_r][1][0]}\frac{dis_2}{dt} + M_{sr[\theta_r][2][0]}\frac{dis_3}{dt} \\
+M_{rr[0][0]}\frac{dir_1}{dt} + M_{rr[0][1]}\frac{dir_2}{dt} + M_{rr[0][2]}\frac{dir_3}{dt} &= \\
-R_{r[0][0]}ir_1 - R_{r[0][1]}ir_2 - R_{r[0][2]}ir_3 \\
-\omega_r(\frac{dM_{sr[\theta_r][0][0]}}{d\theta_r}is_1 + \frac{dM_{sr[\theta_r][1][0]}}{d\theta_r}is_2 + \frac{dM_{sr[\theta_r][2][0]}}{d\theta_r}is_3)
\end{aligned} \tag{32}
$$

$$
\begin{aligned}
M_{sr[\theta_r][0][1]}\frac{dis_1}{dt} + M_{sr[\theta_r][1][1]}\frac{dis_2}{dt} + M_{sr[\theta_r][2][1]}\frac{dis_3}{dt} \\
+M_{rr[1][0]}\frac{dir_1}{dt} + M_{rr[1][1]}\frac{dir_2}{dt} + M_{rr[1][2]}\frac{dir_3}{dt} &= \\
-R_{r[1][0]}ir_1 - R_{r[1][1]}ir_2 - R_{r[1][2]}ir_3 \\
-\omega_r(\frac{dM_{sr[\theta_r][0][1]}}{d\theta_r}is_1 + \frac{dM_{sr[\theta_r][1][1]}}{d\theta_r}is_2 + \frac{dM_{sr[\theta_r][2][1]}}{d\theta_r}is_3)
\end{aligned} \tag{33}
$$

$$
\begin{aligned}
M_{sr[\theta_r][0][2]}\frac{dis_1}{dt} + M_{sr[\theta_r][1][2]}\frac{dis_2}{dt} + M_{sr[\theta_r][2][2]}\frac{dis_3}{dt} \\
+M_{rr[2][0]}\frac{dir_1}{dt} + M_{rr[2][1]}\frac{dir_2}{dt} + M_{rr[2][2]}\frac{dir_3}{dt} &= \\
-R_{r[2][0]}ir_1 - R_{r[2][1]}ir_2 - R_{r[2][2]}ir_3 \\
-\omega_r(\frac{dM_{sr[\theta_r][0][2]}}{d\theta_r}is_1 + \frac{dM_{sr[\theta_r][1][2]}}{d\theta_r}is_2 + \frac{dM_{sr[\theta_r][2][2]}}{d\theta_r}is_3)
\end{aligned} \tag{34}
$$

$$
\frac{d\theta_r}{dt} = \omega_r \tag{35}
$$

$$
\begin{aligned}
\omega_r &= \\
(is_1(\frac{dM_{sr[\theta_r][0][0]}}{d\theta_r}ir_1 + \frac{dM_{sr[\theta_r][0][1]}}{d\theta_r}ir_2 + \frac{dM_{sr[\theta_r][0][2]}}{d\theta_r}ir_3) \\
+is_2(\frac{dM_{sr[\theta_r][1][0]}}{d\theta_r}ir_1 + \frac{dM_{sr[\theta_r][1][1]}}{d\theta_r}ir_2 + \frac{dM_{sr[\theta_r][1][2]}}{d\theta_r}ir_3) \\
+is_3(\frac{dM_{sr[\theta_r][2][0]}}{d\theta_r}ir_1 + \frac{dM_{sr[\theta_r][2][1]}}{d\theta_r}ir_2 + \frac{dM_{sr[\theta_r][2][2]}}{d\theta_r}ir_3) \\
-T_i)/J_m
\end{aligned} \tag{36}
$$

A.2 Expansion in the D/Q (slip) plane

The expansion of equations 4) through 6 is provided in equations 37 through 44 below.

$$\begin{aligned} M_{dq0s[0][0]}\frac{dis_{dqd}}{dt} + M_{dqsr[0][0]}\frac{dir_{dqd}}{dt} = \\ vs_{dqd} - R_{dq0s[0][0]}is_{dqd} - \omega_r(Q_{dq0s[0][1]}is_{dqq} + Q_{dqsr[0][1]}ir_{dqq}) \end{aligned} \tag{37}$$

$$\begin{aligned} M_{dq0s[1][1]}\frac{dis_{dqq}}{dt} + M_{dqsr[1][1]}\frac{dir_{dqq}}{dt} = \\ vs_{dqq} - R_{dq0s[1][1]}is_{dqq} - \omega_r(Q_{dq0s[1][0]}is_{dqd} + Q_{dqsr[1][0]}ir_{dqd}) \end{aligned} \tag{38}$$

$$0 = vs_{dqz} - R_{dq0s[2][2]}is_{dqz} \tag{39}$$

$$\begin{aligned} M^{\intercal}_{dqsr[0][0]}\frac{dis_{dqd}}{dt} + M_{dqr[0][0]}\frac{dir_{dqd}}{dt} = \\ -R_{dqr[0][0]}ir_{dqd} \end{aligned} \tag{40}$$

$$\begin{aligned} M^{\intercal}_{dqsr[1][1]}\frac{dis_{dqq}}{dt} + M_{dqr[1][1]}\frac{dir_{dqq}}{dt} = \\ -R_{dqr[1][1]}ir_{dqq} \end{aligned} \tag{41}$$

$$\begin{aligned} M_{dqr[2][2]}\frac{dir_{dqz}}{dt} = \\ -R_{dqr[2][2]}ir_{dqz} \end{aligned} \tag{42}$$

$$\frac{d\theta_r}{dt} = \omega_r \tag{43}$$

$$\begin{aligned} \omega_r = \\ (.5Q_{dqsr[0][1]}is_{dqd}ir_{dqq} + .5Q_{dqsr[1][0]}is_{dqq}ir_{dqd} \\ +.5Q^{\intercal}_{dqsr[0][1]}is_{dqq}ir_{dqd} + .5Q^{\intercal}_{dqsr[1][0]}is_{dqd}ir_{dqq} \\ -T_i)/J_m \end{aligned} \tag{44}$$

A.3 Expansion in the Synchronous D/Q plane

The expansion of equations 7) through 9 is provided in equations 45 through 52 below.

$$\begin{aligned} M_{sync0s[0][0]}\frac{dis_{sdqd}}{dt} + M_{syncsr[0][0]}\frac{dir_{sdqd}}{dt} = \\ vs_{sdqd} - R_{sync0s[0][0]}is_{sdqd} \\ -\omega_r(Q_{sync0s[0][1]}is_{sdqq} + Q_{syncsr[0][1]}ir_{sdqq}) \\ -(\omega_r - \omega_s)(Q_{syncd0s[0][1]}is_{sdqq} + Q_{syncdsr[0][1]}ir_{sdqq}) \end{aligned} \tag{45}$$

$$\begin{aligned} M_{sync0s[1][1]}\frac{dis_{sdqq}}{dt} + M_{syncsr[1][1]}\frac{dir_{sdqq}}{dt} = \\ vs_{sdqq} - R_{sync0s[1][1]}is_{sdqq} \\ -\omega_r(Q_{sync0s[1][0]}is_{sdqd} + Q_{syncsr[1][0]}ir_{sdqd}) \\ -(\omega_r - \omega_s)(Q_{syncd0s[1][0]}is_{sdqd} + Q_{syncdsr[1][0]}ir_{sdqd}) \end{aligned} \tag{46}$$

$$0 = vs_{sdqz} - R_{sync0s[2][2]}is_{sdqz} \tag{47}$$

$$\begin{aligned} M^{\intercal}_{syncsr[0][0]}\frac{dis_{sdqd}}{dt} + M_{syncr[0][0]}\frac{dir_{sdqd}}{dt} = \\ -R_{syncr[0][0]}ir_{sdqd} \\ -(\omega_r - \omega_s)(Q^{\intercal}_{syncdsr[0][1]}is_{sdqq} + Q_{syncdr[0][1]}ir_{sdqq}) \end{aligned} \tag{48}$$

$$\begin{aligned} M^{\intercal}_{syncsr[1][1]}\frac{dis_{sdqq}}{dt} + M_{syncr[1][1]}\frac{dir_{sdqq}}{dt} = \\ -R_{syncr[1][1]}ir_{sdqq} \\ -(\omega_r - \omega_s)(Q^{\intercal}_{syncdsr[1][0]}is_{sdqd} + Q_{syncdr[1][0]}ir_{sdqd}) \end{aligned} \tag{49}$$

$$M_{syncr[2][2]}\frac{dir_{sdqz}}{dt} = -R_{syncr[2][2]}ir_{sdqz} \tag{50}$$

$$\frac{d\theta_r}{dt} = \omega_r \tag{51}$$

$$\begin{aligned} \omega_r = \\ (.5S_{syncsr[0][1]}is_{sdqd}ir_{sdqq} + .5S_{syncsr[1][0]}is_{sdqq}ir_{sdqd} \\ +.5S^{\intercal}_{syncsr[0][1]}is_{sdqq}ir_{sdqd} + .5S^{\intercal}_{syncsr[1][0]}is_{sdqd}ir_{sdqq} \\ -T_i)/J_m \end{aligned} \tag{52}$$

B Simulation Plots

Finally, some simulation plots are presented to support the information provide above. First some details on how the open loop voltage was generated for the simulations presented in this paper as well as the modifications made to the D/Q and Synchronous transformations presented by **Roberts** to make them usable for the single stator induction motor described in this paper.

One point to make here is that a formal simulation in the D/Q (slip) plane was skipped. This is because the the D/Q and Synchronous transformations (with their inverses) mentioned in the next section can be applied in the Rotating or Synchronous D/Q planes to obtain any information that is required in the D/Q (slip) plane.

B.1 Background Information

The generation of the stator angular velocity and voltage used in all simulations presented in this paper are defined by Equations 53 and 54 below.

$$\begin{array}{r} \omega_s = \\ .5VO\_TRAJ(sin(t\pi/RT\_TRAJ - \pi/2) + 1) \\ \underline{if(t < RT\_TRAJ), else} \\ VO\_TRAJ \\ \underline{if(t < RT\_TRAJ + CT\_TRAJ), else} \\ .5VO\_TRAJ(sin((CT\_TRAJ + 2RT\_TRAJ - t)\pi/RT\_TRAJ - \pi/2) + 1) \\ \underline{if(t < 2RT\_TRAJ + CT\_TRAJ), else} \\ 0 \end{array} \tag{53}$$

$$\begin{aligned} vs_1 &= .5\omega_s DC\_BUS\_VOLTAGEcos(.5\theta_s)/VO\_TRAJ \\ vs_2 &= .5\omega_s DC\_BUS\_VOLTAGEcos(.5\theta_s - \frac{2\pi}{3})/VO\_TRAJ \\ vs_3 &= .5\omega_s DC\_BUS\_VOLTAGEcos(.5\theta_s - \frac{4\pi}{3})/VO\_TRAJ \end{aligned} \tag{54}$$

The total run time is defined by $2RT\_TRAJ + CT\_TRAJ$ with RT_TRAJ set to 4 seconds and CT_TRAJ set to 2 seconds. VO_TRAJ is set to 100 radians/sec. The bus voltage $DC\_BUS\_VOLTAGE$ is set to 600 VDC. θ_s is derived from the integral of the stator angular velocity ω_s defined by Equation 53.

The various transformations defined by **Roberts** that are used in the plots that follow are provided below.

Equations 55 and 56 are used to transform Equation 54 so as to derive the voltage for the Synchronous D/Q simulation model defined by Equations 45 through 52 above[2].

$$\begin{bmatrix} vs_{dqd} \\ vs_{dqq} \\ vs_{dqz} \end{bmatrix} = \sqrt{\frac{2}{3}} \begin{bmatrix} \cos\theta_r & cos(\theta_r - \frac{2\pi}{3}) & cos(\theta_r - \frac{4\pi}{3}) \\ \sin\theta_r & sin(\theta_r - \frac{2\pi}{3}) & sin(\theta_r - \frac{4\pi}{3}) \\ \frac{1}{\sqrt{2}} & \frac{1}{\sqrt{2}} & \frac{1}{\sqrt{2}} \end{bmatrix} \begin{bmatrix} vs_1 \\ vs_2 \\ vs_3 \end{bmatrix} \tag{55}$$

$$\begin{bmatrix} vs_{sdqd} \\ vs_{sdqq} \\ vs_{sdqz} \end{bmatrix} = \begin{bmatrix} cos(\theta_r - \theta_s) & sin(\theta_r - \theta_s) & 0 \\ -sin(\theta_r - \theta_s) & cos(\theta_r - \theta_s) & 0 \\ 0 & 0 & 1 \end{bmatrix} \begin{bmatrix} vs_{dqd} \\ vs_{dqq} \\ vs_{dqz} \end{bmatrix} \tag{56}$$

Equations 57 and 58 are used when translating from the rotating plane to the synchronous D/Q plane[3].

$$\begin{bmatrix} is_{dqd\_derived} \\ is_{dqq\_derived} \\ is_{dqz\_derived} \end{bmatrix} = \sqrt{\frac{2}{3}} \begin{bmatrix} \cos\theta_r & cos(\theta_r - \frac{2\pi}{3}) & cos(\theta_r - \frac{4\pi}{3}) \\ \sin\theta_r & sin(\theta_r - \frac{2\pi}{3}) & sin(\theta_r - \frac{4\pi}{3}) \\ \frac{1}{\sqrt{2}} & \frac{1}{\sqrt{2}} & \frac{1}{\sqrt{2}} \end{bmatrix} \begin{bmatrix} is_1 \\ is_2 \\ is_3 \end{bmatrix} \tag{57}$$

$$\begin{bmatrix} is_{sdqd\_derived} \\ is_{sdqq\_derived} \\ is_{sdqz\_derived} \end{bmatrix} = \begin{bmatrix} cos(\theta_r - \theta_s) & sin(\theta_r - \theta_s) & 0 \\ -sin(\theta_r - \theta_s) & cos(\theta_r - \theta_s) & 0 \\ 0 & 0 & 1 \end{bmatrix} \begin{bmatrix} is_{dqd\_derived} \\ is_{dqq\_derived} \\ is_{dqz\_derived} \end{bmatrix} \tag{58}$$

[2] Equation 55 alone places the voltage in the D/Q (Slip) plane
[3] Equation 57 alone places the current in the D/Q (Slip) plane

Equations 59 and 60 are used when translating from the synchronous D/Q plane to the rotating plane[4] .

$$\begin{bmatrix} is_{dqd\_derived} \\ is_{dqq\_derived} \\ is_{dqz\_derived} \end{bmatrix} = \begin{bmatrix} cos(\theta_r - \theta_s) & -sin(\theta_r - \theta_s) & 0 \\ sin(\theta_r - \theta_s) & cos(\theta_r - \theta_s) & 0 \\ 0 & 0 & 1 \end{bmatrix} \begin{bmatrix} is_{sdqd} \\ is_{sdqq} \\ is_{sdqz} \end{bmatrix} \tag{59}$$

$$\begin{bmatrix} is_{1\_derived} \\ is_{2\_derived} \\ is_{3\_derived} \end{bmatrix} = \sqrt{\frac{2}{3}} \begin{bmatrix} \cos\theta_r & \sin\theta_r & \frac{1}{\sqrt{2}} \\ cos(\theta_r - \frac{2\pi}{3}) & sin(\theta_r - \frac{2\pi}{3}) & \frac{1}{\sqrt{2}} \\ cos(\theta_r - \frac{4\pi}{3}) & sin(\theta_r - \frac{4\pi}{3}) & \frac{1}{\sqrt{2}} \end{bmatrix} \begin{bmatrix} is_{dqd\_derived} \\ is_{dqq\_derived} \\ is_{dqz\_derived} \end{bmatrix} \tag{60}$$

[4]Equation 59 alone places the current in the D/Q (Slip) plane

B.2 Results of Simulation in the Rotating Frame

The plots provided in this section were produced by the simulation model described by Equations 29 through 36 of Section A.1.

Voltages vs_1, vs_2 and vs_3 are generated by Equation 54. Voltage vs_1 is shown in Figure 6 below.

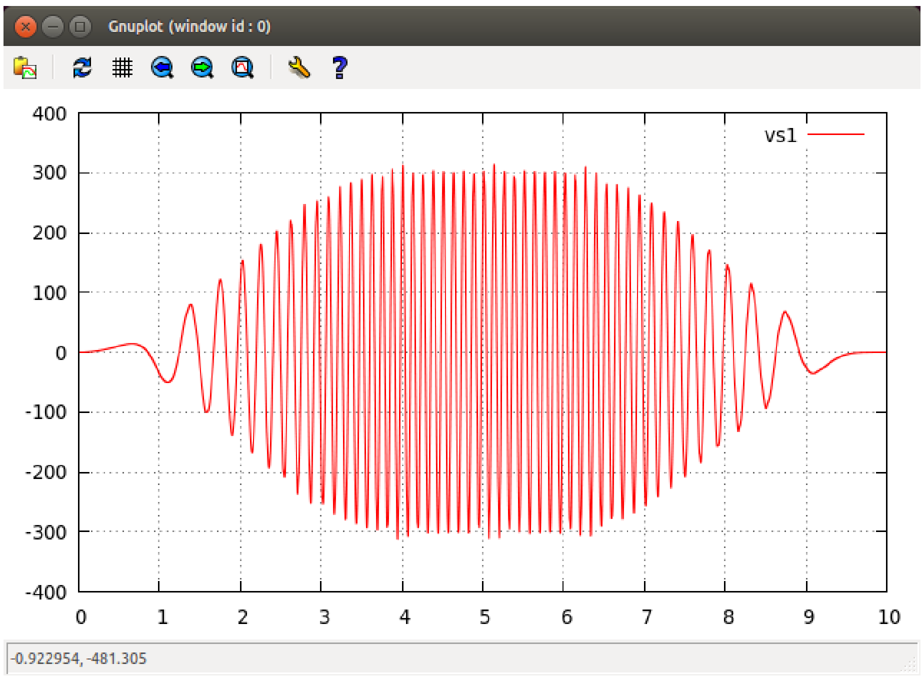

Figure 6: Phase 1 voltage vs_1 of a 3-phase supply voltage applied to the motor for all open loop tests (vs_2 and vs_3 are not shown).

The results for stator current is_1 and rotor current ir_2 are shown in Figures 7 and 8.

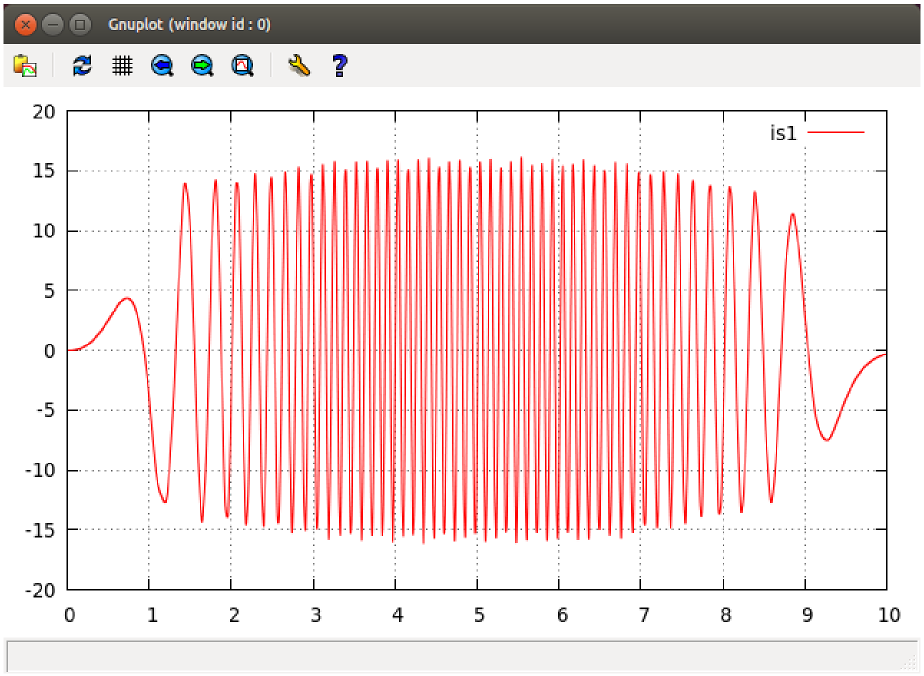

Figure 7: Corresponding Phase 1 stator current is_1 for the applied open loop voltage shown in Figure 6 above (is_2 and is_3 are not shown).

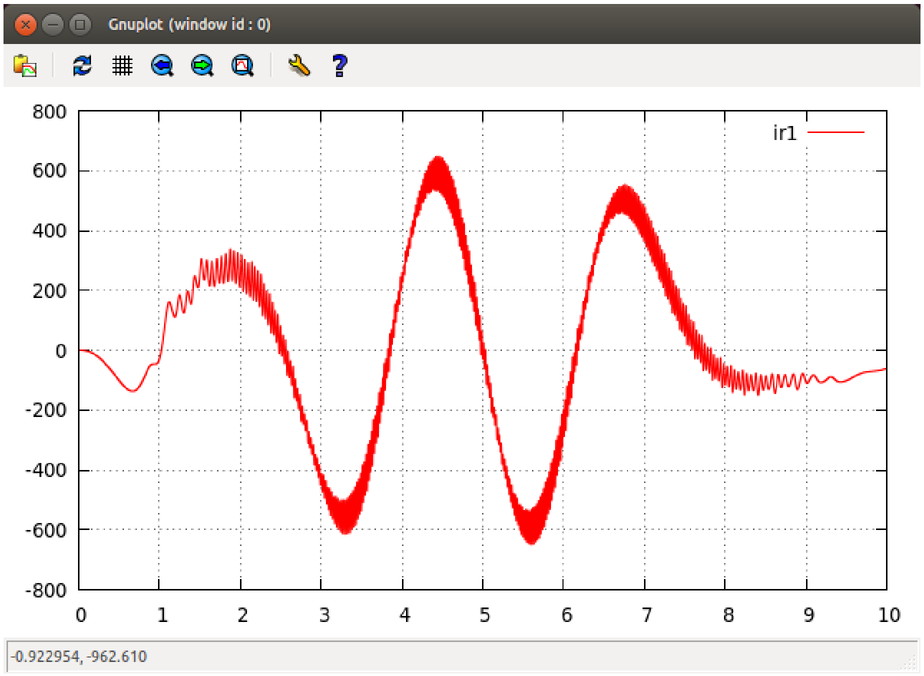

Figure 8: Corresponding Phase 1 rotor bar current ir_1 for the applied open loop voltages shown in Figure 6 above (ir_2 and ir_3 not shown).

Note in Figure 8 the excessive ripple caused by applying the sinusoidal voltages of vs_1, vs_2 and vs_3 to the non-sinusoidally wound stator of the simplistic induction motor described in Section 2.

Next, a plot of the D/Q (Slip) stator currents derived from the rotating (terminal) plane stator currents is_1, is_2 and is_3.

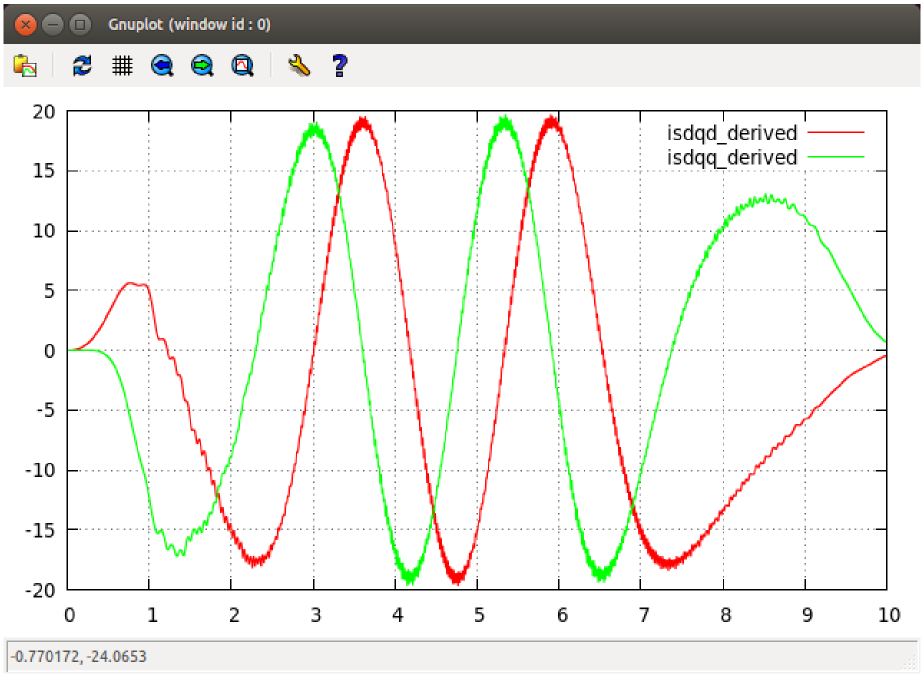

Figure 9: Transformation of is_1, is_2 and is_3 into the D/Q (Slip) plane using the transformations described in Equation 57 above (is_{dqz} not shown).

The plot of Figure 9 is derived by applying the transformation described by 57 to is_1, is_2 and is_3.

Next, the currents in the Synchronous D/Q plane *derived from the derived* D/Q (Slip) currents.

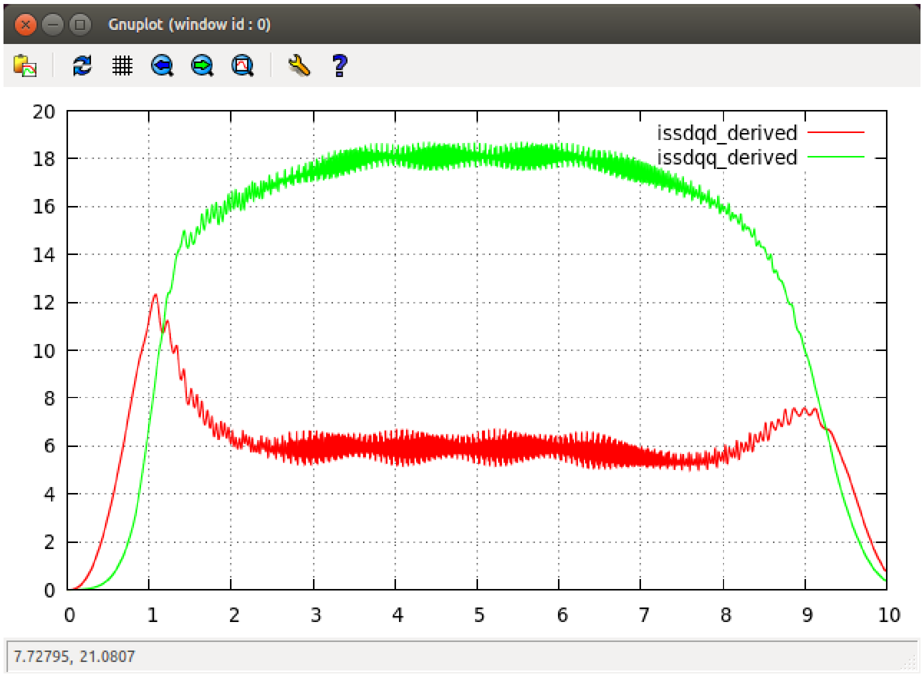

Figure 10: Transformation of $isdqd$, $isdqq$ and $isdqz$ into the Synchronous D/Q plane using the transformation described by Equation 58 above (is_{sdqz} not shown).

The plot of Figure 10 is derived by applying the transformation described by 57 followed by 58 to is_1, is_2 and is_3.

And finally, a plot of the stator driving frequency and resultant rotor frequency with a closeup view showing the torque ripple. Because the simulation involves a 2-Pole motor, the physical shaft frequency and stator voltage frequency are the same.

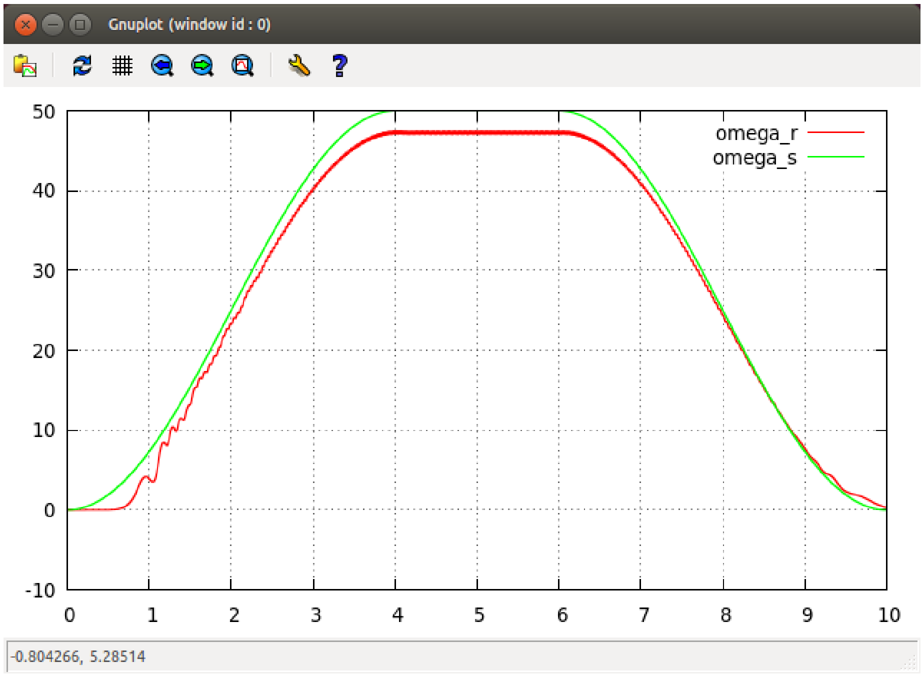

Figure 11: Rotor speed ω_r vs ω_s. ω_r is produced by Equation 36 with ω_s is produced by Equation 53.

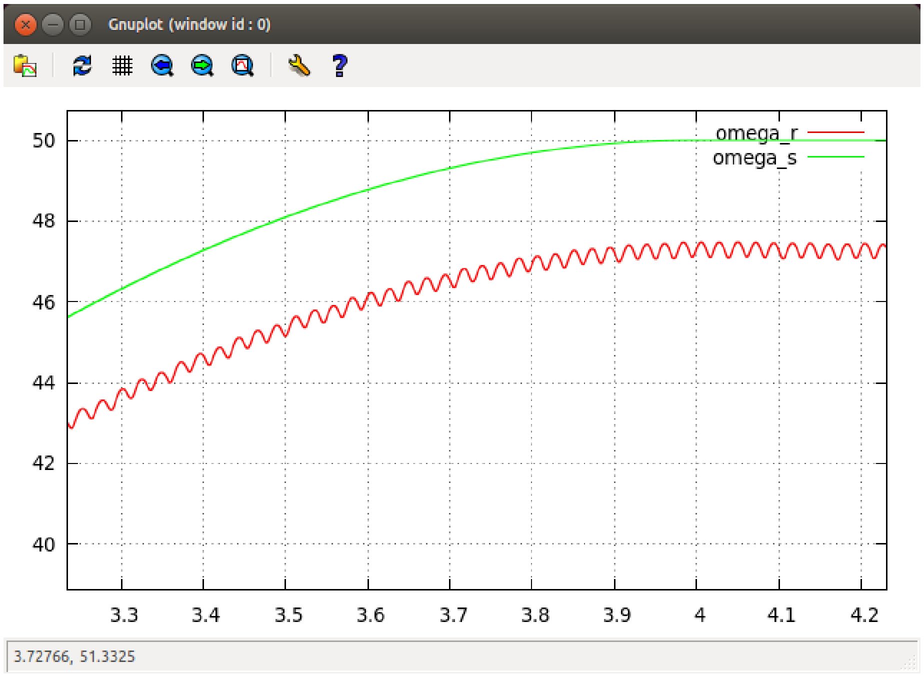

Figure 12: Close-up of Figure 11 above.

Note in Figure 12 the torque ripple effects on ω_r caused by the non-sinusoidal wound stator of the simplistic induction motor described in Section 2.

B.3 Results of Simulation in the Synchronous D/Q Frame

The plots provided in this section were produced by the simulation model described by Equations 45 through 52 of Section A.3.

First the driving voltages vs_{sdqd} and vs_{sdqq} in the Synchronous D/Q plane[5].

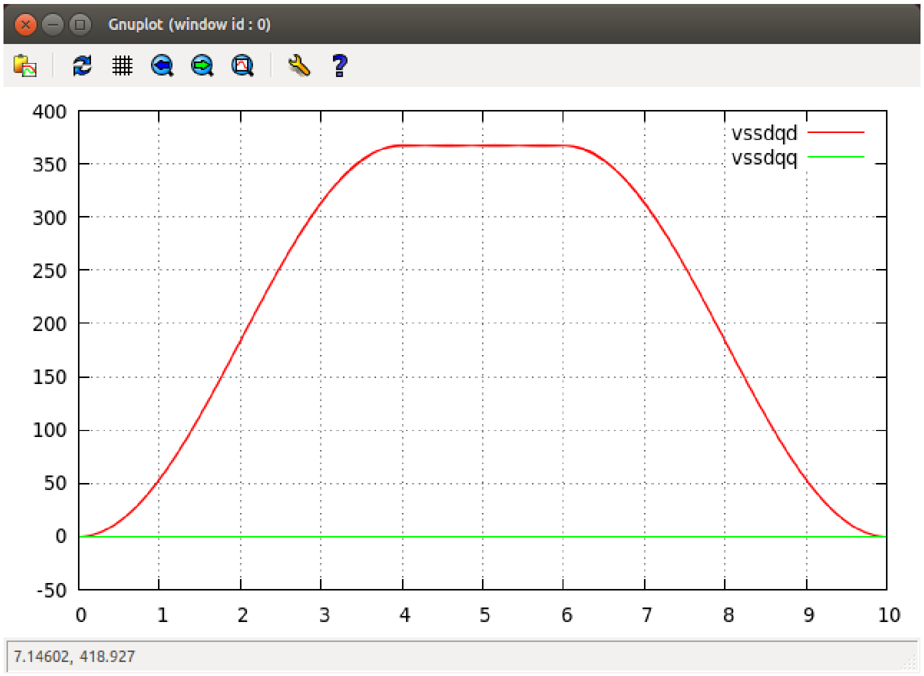

Figure 13: D/Q voltages vs_{sdqd} and vs_{sdqq} in the synchronous D/Q plane. These are generated from vs_1, vs_2 and $vs3$ using Equations 55 and 56 above.

It should be noted that the voltage generation Equations 53 and 54 produces a command where all voltage is placed in the *direct* (vs_{sdqd}) with the *quadrature* (vs_{sdqq}) set to zero. This is because we are doing all simulations under open loop conditions. In an actual control environment, voltages would be generated such that the *quadrature* component would control torque with the option of field weakening controlled by the *direct* component.

Next, the resultant stator currents in the Synchronous D/Q plane.

[5]In this paper, I may interchange the words *frame* and *plane*.

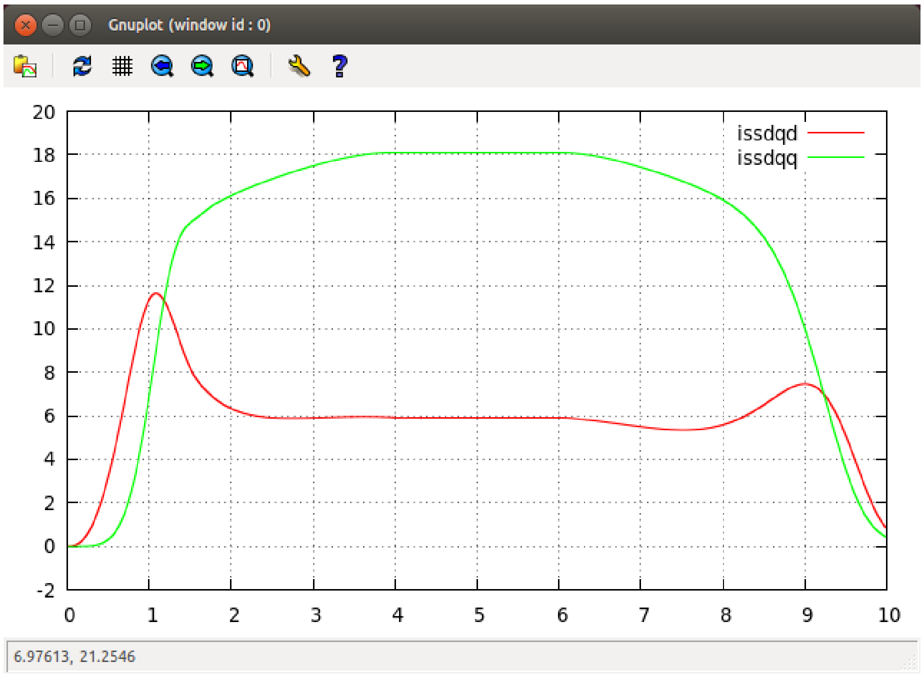

Figure 14: Synchronous D/Q stator currents is_{sdqd} and is_{sdqq} for the applied open loop voltages shown in Figure 13 above (is_{sdqz} is zero and is not shown).

It should be noted that Figure 14 produced by the simulation running in the synchronous D/Q plane and Figure 10 produce by the simulation running in the rotating (or terminal) reference plane and then translated by transformations 57 and 58, produce identical results (except for the removal of the torque ripple effects that are not modeled when running the simulation in the synchronous D/Q plane).

Like what was done for the simulation in the Rotating plane, we can transform the currents shown in Figure 14 back to the Rotating plane as shown in the next plot.

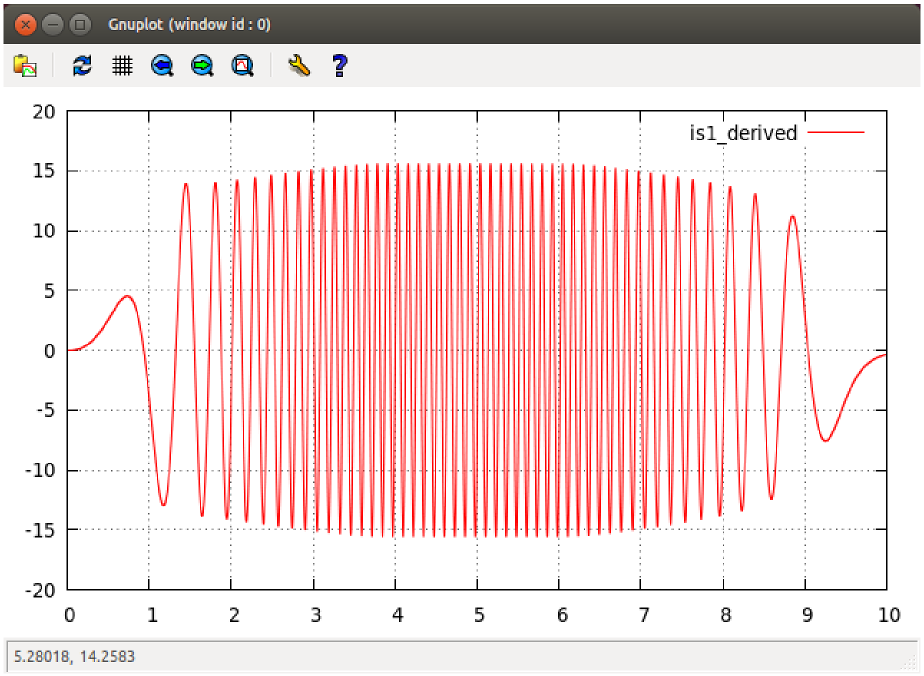

Figure 15: Synchronous D/Q stator currents is_{sdqd} and is_{sdqq} translated back to the rotating plane using Equations 59 and 60 ($is_{2\_derived}$ and $is_{3\_derived}$ not shown).

And finally, a plot of the stator driving frequency and resultant rotor frequency created in the Synchronous D/Q plane.

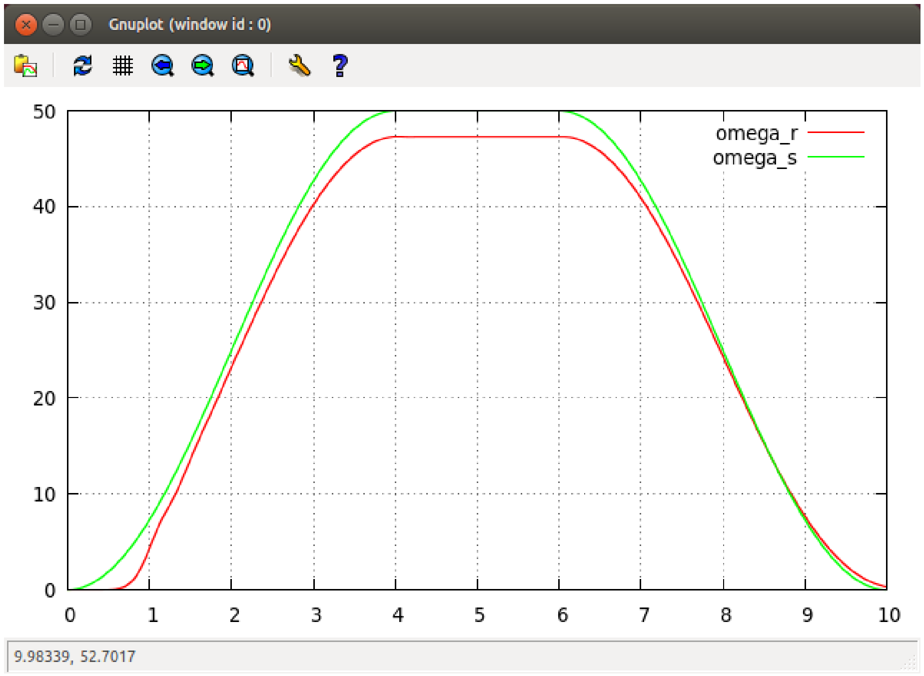

Figure 16: Rotor speed ω_r vs ω_s. ω_r is produced by Equation 52 with ω_s is produced by Equation 53.

The results in Figure 16 are virtually identical to that that shown in Figure 11 above again noting that the torque ripple effects are absent when simulating in the Synchronous D/Q plane.

B.4 Simulations to validate control strategies

Document [4] describes in detail the simulator used to generate the data presented in this paper. Along with a sixth order Runge-Kutta ODE solver to handle the real time execution of the motor model, the simulator possesses the ability to simulate control processes that would normally be executed in an interrupt routine on the control processor or DSP. This is called a a **CtrlObject** and in the case of this simulation, is setup to run every 50 uSec.

Three tests using this control object are presented below. For each of these tests, selected states are read from the simulator and applied to the specific algorithm to be verified.

B.4.1 Test 1: Solve for Synchronous D/Q Stator Currents using Euler method running in a CtrlObject

Roberts suggests some control strategies for the induction motor in Chapter 7 and Chapter 8 of his paper. Common to all but two of the methods mentioned is a requirement to have a running model of the electrical equations for the induction motor. For our simple example in this paper, this is the model described by Equation 14.

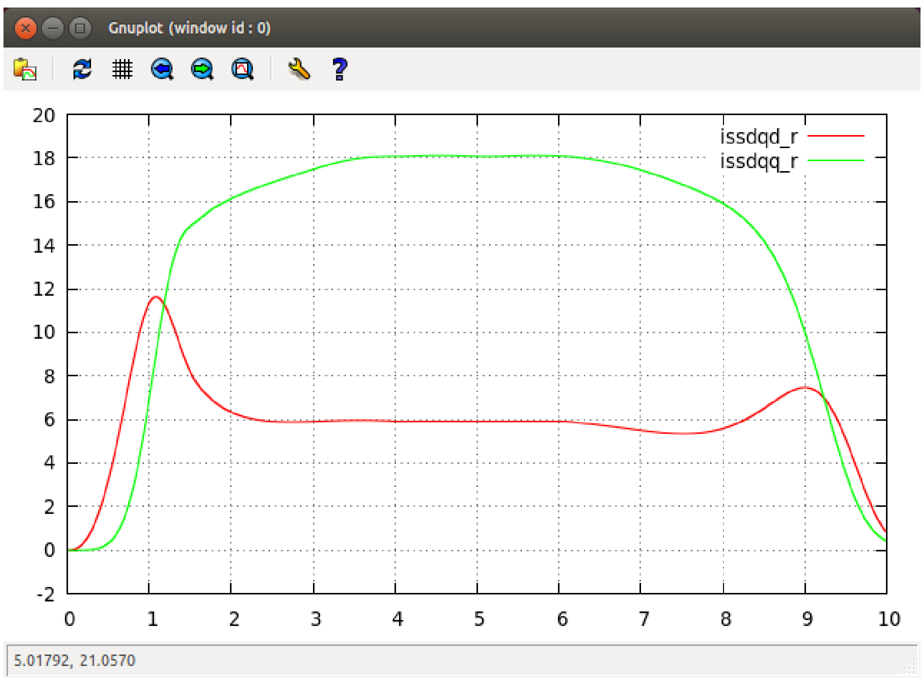

Figure 17: Results of a test showing a derived form of the synchronous D/Q currents is_{sdqd} and is_{sdqq} produced by applying the values ω_r, ω_s, vs_{sdqd} and vs_{sdqq} of the simulation run shown described in section B.3 above to Equation 14 running in the **CtrlObject**.

Equation 14 is setup to run using the a simple Euler method (first order integration) with an incremental step size of 50 uSec executed concurrently with the simulation run. These derived currents are labeled is_{sdqd_r} and is_{sdqq_r}. The point here is to show that an embedded DSP algorythm can derive accurately (given an accurate model) the actual Synchronous D/Q currents for the proposes of generating reference currents. Compare these plots shown in Figure 17 with Figure 14.

A close-up view of 17 is shown in the next figure.

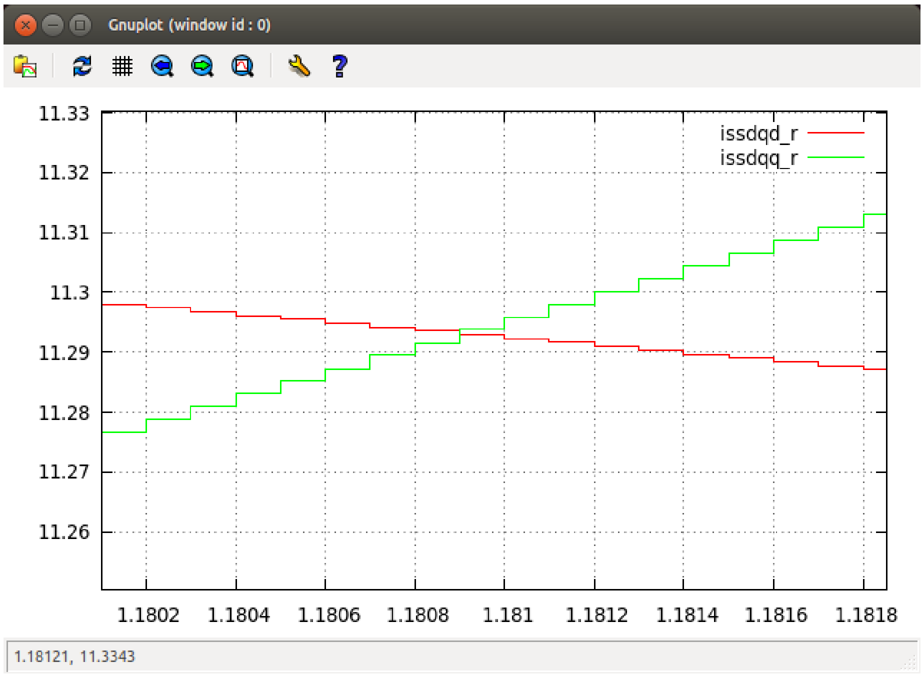

Figure 18: This is close-up of Figure 17 above showing the incremental step size of 50 uSec produced by the Euler method running in the **CtrlObject**.

B.4.2 Test 2: Solve for Synchronous D/Q stator voltages running in a CtrlObject

Roberts derives in Equation 8.14 page 213 of his paper a way to determine the appropriate stator voltages to be applied to the motor given the stator current and flux. Here we apply his analysis to our simple motor. It should be noted that we disregard his transformation used to convert stator and rotor currents to a controllable stator flux (see Equation 8.5 and 8.6 page 212 of **Roberts**).

Instead we input the rotor currents directly from the simulator.

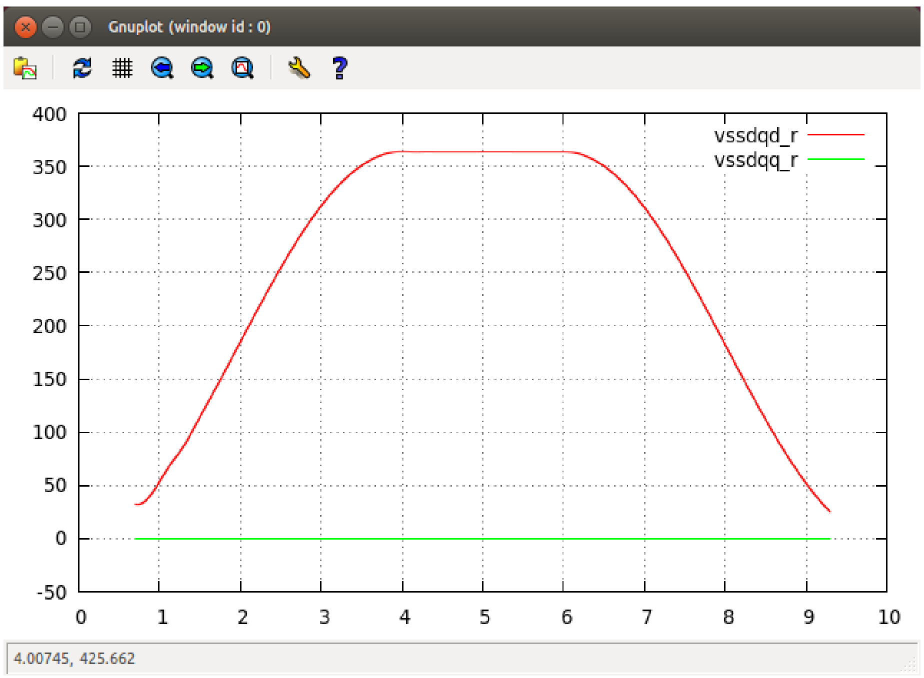

Figure 19: Results of a test to provide a verification for Equation 8.14, page 213 of **Roberts** which has been reduced in this paper to that described by Equation 19.

The implementation here is similar to that used to derive the results in Figures 17 and 18 above.

Equation 19 is solved for vs_{sdqd} with vs_{sdqq} set to zero. The values for is_{sdqd}, is_{sdqq}, ir_{sdqd}, ir_{sdqq}, ω_r and ω_s are gathered while running the simulation described in section B.3 and plugged into 19. This produces vs_{sdqd_r}. Compare this derived value for vs_{sdqd} with that shown in Figure 13. They are essentially identical.

B.4.3 Test 3: Solve for Synchronous D/Q stator voltages using a Lagrange approach running in a CtrlObject

As pointed out by **Roberts** in his description for Equation 8.14 of page 213, there are an infinite number of valid solution for this equation when determining the values for vs_{sdqd} and vs_{sdqq} There is also a problem with determining a valid value for the stator frequency variable ω_s. Roberts does not elaborate on what he terms the *...the solution giving the minimum value.* I believe what he is referring to is a Lagrange solution based on the constraint that both vs_{sdqq} and vs_{sdqd} are held to a minimum. This technique is used by [2] for the control of an AC brushless permanent magnet motor.

In a practical sense, I point out in [4] that this technique for determining vs_{sdqq} and vs_{sdqd} is in my opinion flawed because it disregards the side effects of excessive current draw on the amplifier for the sake of keeping the magnitude of the of *sum-of-squares* of the applied stator voltage to a minimum at any operating point of the motor.

I believe a better method is to use the minimization technique above but instead set vs_{sdqd} to zero and solve for vs_{sdqq} and ω_s. Then in the actual control environment vs_{sdqd} is controlled by some independent process for the purpose of optimizing the motor field (field weakening based on motor speed)[6]

The Lagrange is defined using Equations 20 through 28 above. In the actual test which is shown below, I set vs_{sdqq} to zero and solve for vs_{sdqd} and ω_s. As discussed above, this was done because the open loop simulation run shown in Section B.3 produced by applying Equations 55 and 56 to Equations 53 and 54 generates a voltage vector entirely in the synchronous *d-plane.*

This is shown in Figures 20 and 21 below.

[6] One thing that needs to be address using this approach is the fact that we invalidate the Lagrange when we set vs_{sdqd} to a value other then zero.

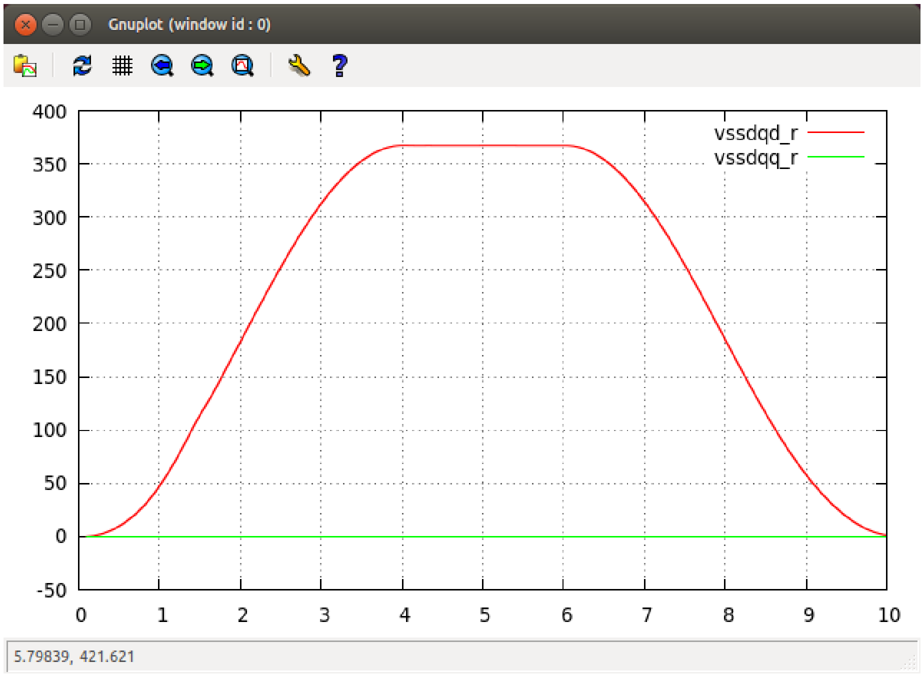

Figure 20: Results of a test used to provide a verification for 20 through 28 above to solve for vs_{sdqd}.

The implementation here is similar to that used in the descriptions for Sections B.4.1 and B.4.2 above. The values for is_{sdqd}, is_{sdqq}, ir_{sdqd}, ir_{sdqq}, vs_{sdqq} (set to zero) and ω_r are gathered while running the simulation described in section B.3. This produces vs_{sdqd_r}. Compare this derived value for vs_{sdqd} in Figure 20 with that shown in Figure 13. They are essentially identical.

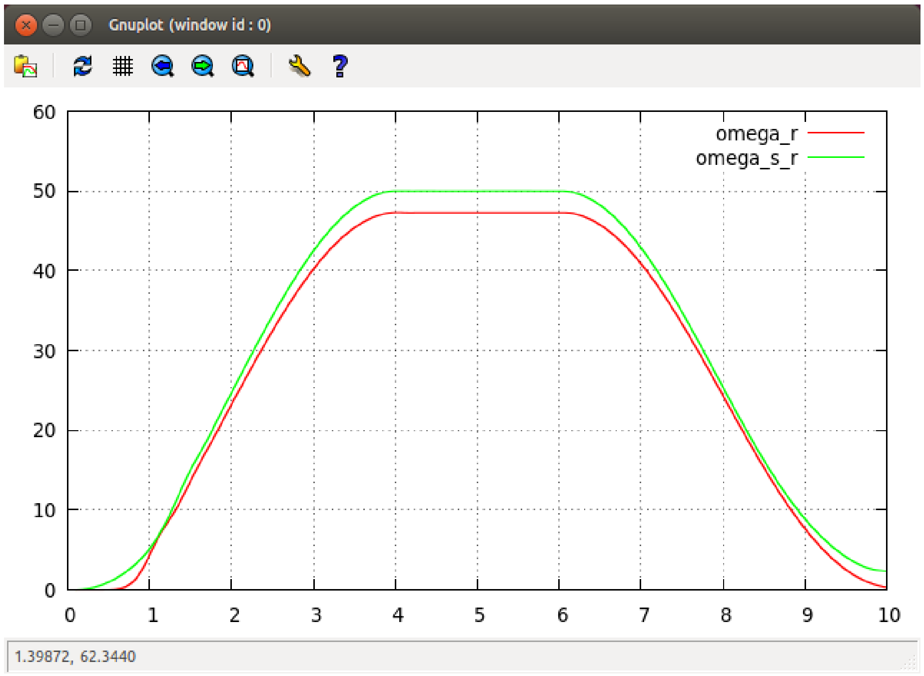

Figure 21: Results of a test used to provide a verification for 20 through 28 above to solve for ω_s.

Like Figure 20 above the Lagrange defined by 20 through 28 are used to determine the optimum value for ω_s. Again, the values for is_{sdqd}, is_{sdqq}, ir_{sdqd}, ir_{sdqq}, vs_{sdqq} (set to zero) and ω_r are gathered while running the simulation described in section B.3. This produces ω_{s_r} (which is plotted with ω_r). Compare this derived value for ω_{s_r} in Figure 21 with that shown for ω_s in Figure 16. They are essentially identical.

References

[1] Paul C. Roberts
A Study of Brushless Doubly-Fed Induction Machines.
Emmanuel College, University of Cambridge
https://meaconsultingdotorg.files.wordpress.com/2015/12/roberts_bdfm_dissertation_2005.pdf

[2] Marc Bodson, John N. Chiasson, Robert T. Novotnak and Ronold B. Rekoswski
High Performance Nonlinear Feedback Control of a Permanent Magnet Stepping Motor.
First IEEE Conference on Control Applications, 1992. ISBN 0-7803-0047-5.

[3] Marsden, Thromba
Vector Calculus
Second Edition, W.H. Freeman and Company, 1976. ISBN 0-7167-1244-X
Section 4.3 *Constrained Extrema and Lagrange Multipliers*

[4] *Implementation of an Advanced AC Brushless Motor Controller for Use in High Reliability Applications*
Michael E. Aiello, April 2 2016.
https://meaconsultingdotorg.files.wordpress.com/2015/12/controller.pdf